

At the steady state (resting membrane) when there is not net current:

$$I_K + I_{Na} + I_{Cl} = 0$$

For K, Na and Cl:

$$I_K = g_K(E_m - E_K)$$

$$I_{Na} = g_{Na}(E_m - E_{Na})$$

$$I_{Cl} = g_{Cl}(E_m - E_{Cl})$$

$$\therefore E_m = \frac{g_K E_K}{\sum g} + \frac{g_{Na} E_{Na}}{\sum g} + \frac{g_{Cl} E_{Cl}}{\sum g}$$

Where $\sum g = g_K + g_{Na} + g_{Cl}$

An action potential recorded intracellularly from a squid giant axon. The vertical scale shows the potential (mV) of the internal electrode with respect to the external sea water. The action potential is preceded by small stimulus artefact. The sine wave at the bottom is a time marker, frequency 500 Hz. (From Hodgkin and Huxley, 1945.)

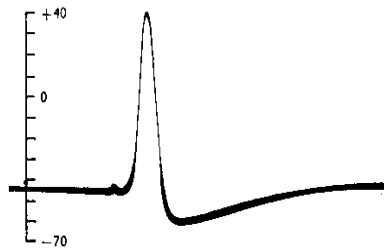
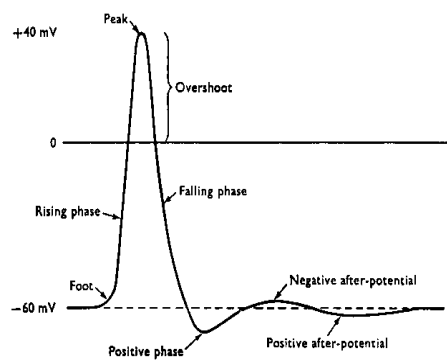


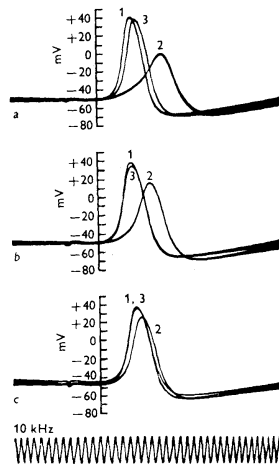
Diagram to show the nomenclature applied to an action potential and the after-potentials which follow it.

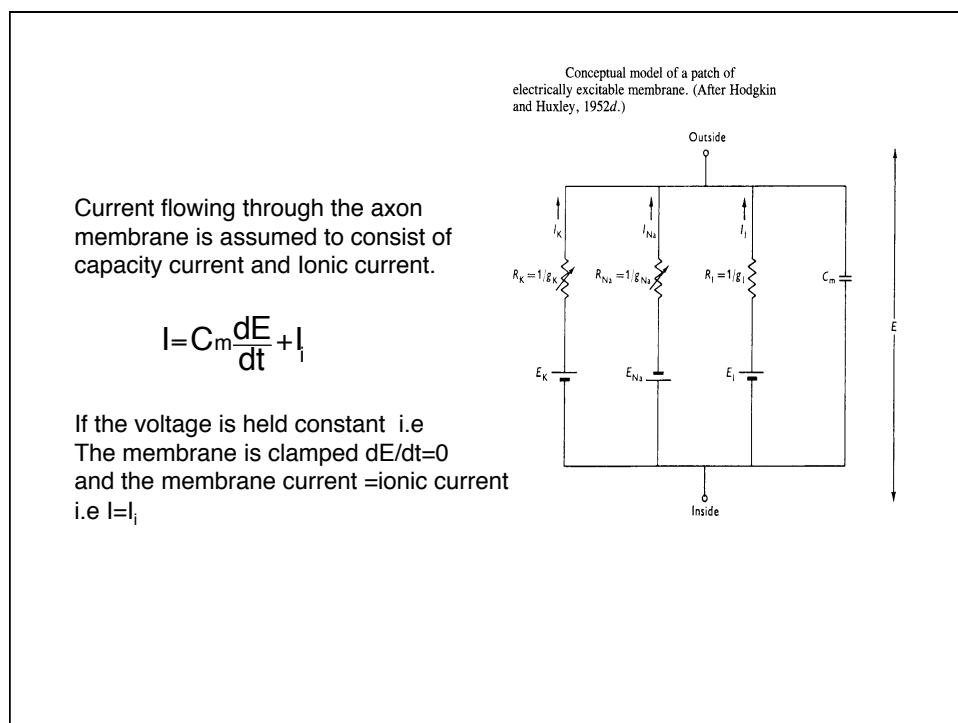
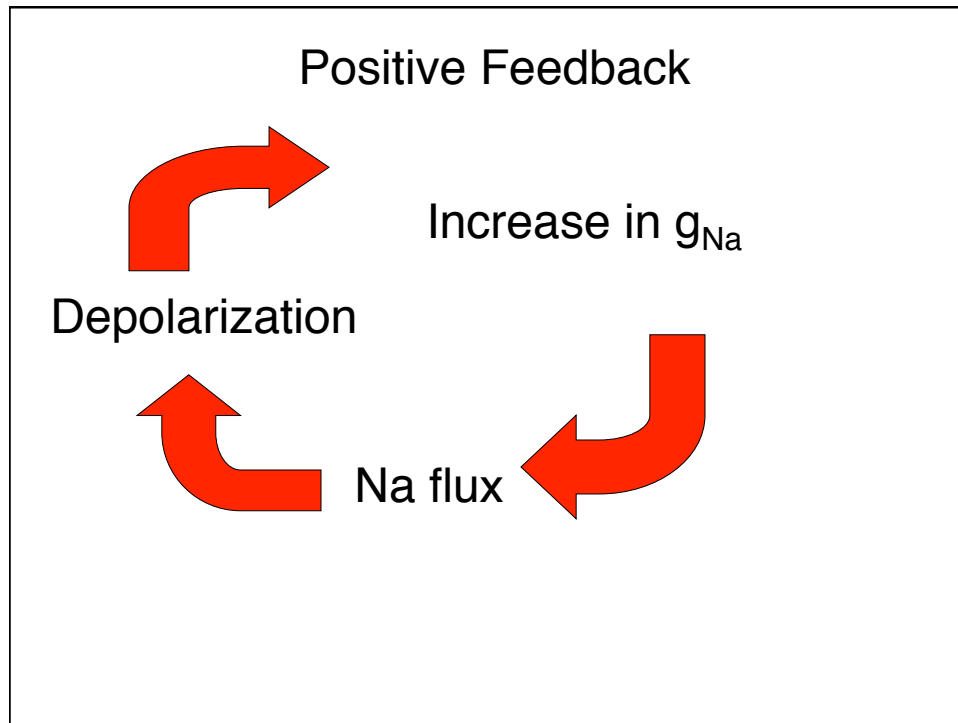


The "sodium theory" of the action potential

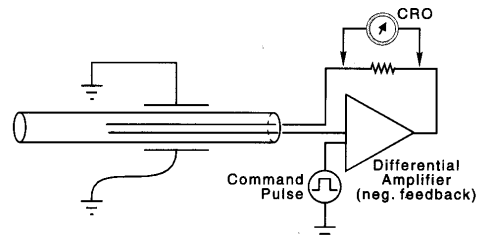
Action potentials exhibit an overshoot. Thus the peak of the action potential is well above zero. Hodgkin and Katz suggested (in 1949) that this was due to a rapid and selective increase in the permeability towards sodium. Thus g_{Na} transiently becomes much greater than g_K . How can this idea be tested?

The effect of reducing the external sodium ion concentration on the size of the action potential in a squid giant axon. In each set of records, record 1 shows the response with the axon in sea water, record 2 in the experimental solution, and record 3 in sea water again. Experimental solutions were made by mixing sea water and isotonic glucose solutions, the proportions of sea water being *a*, 33%; *b*, 50%; and *c*, 70%. (From Hodgkin and Katz, 1949.)



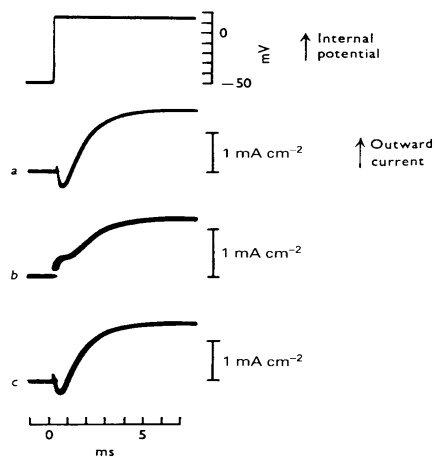


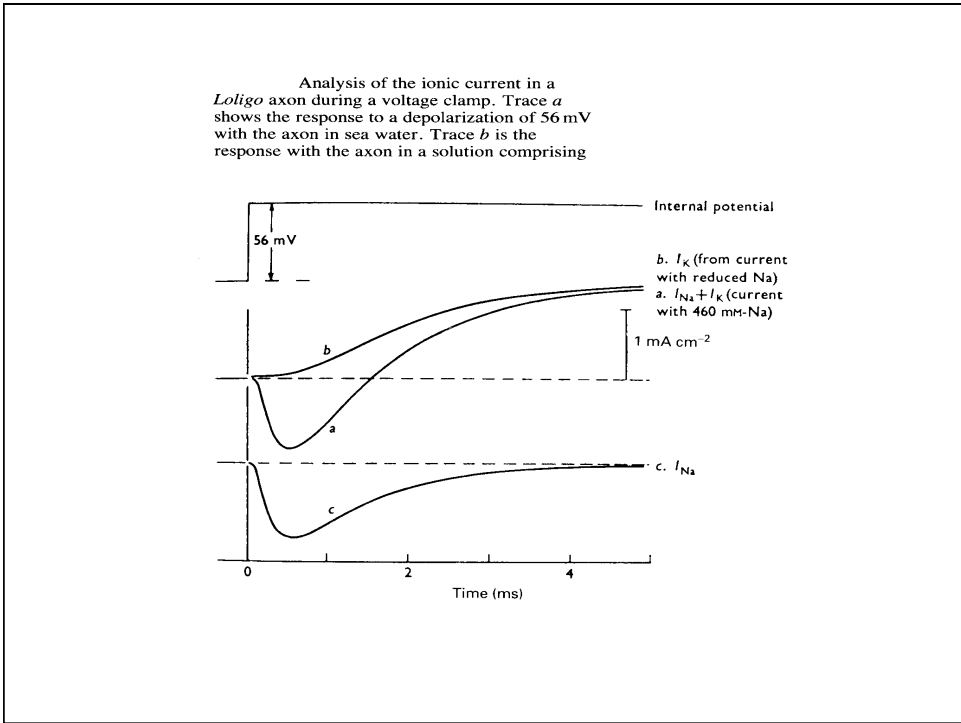
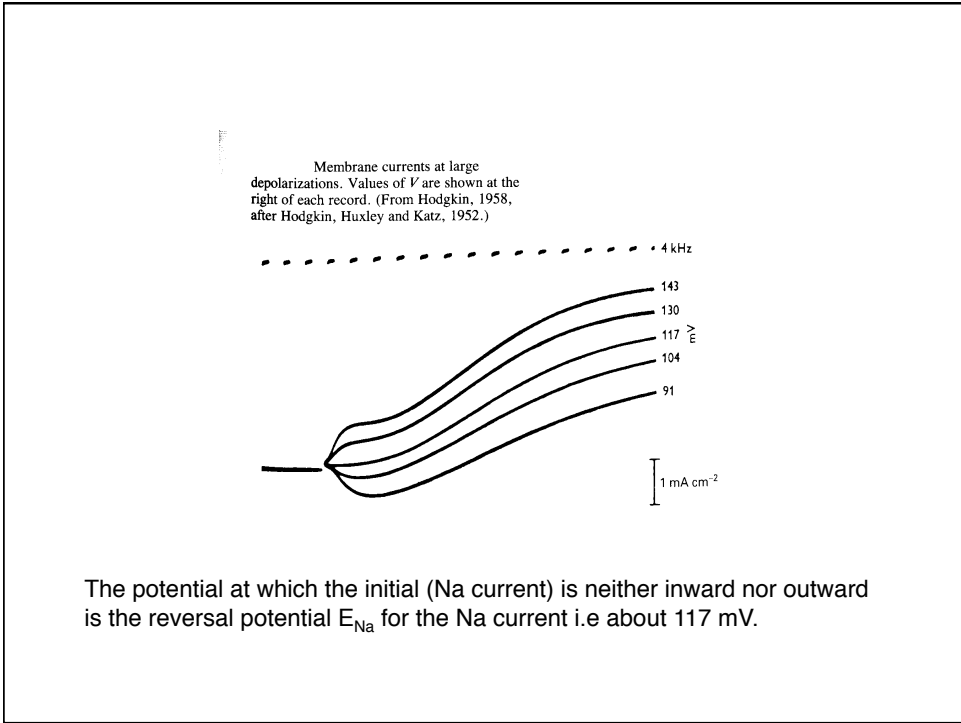
Voltage Clamp

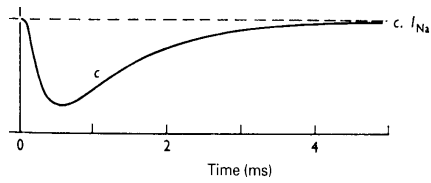


The voltage clamp method used in a squid giant axon. The two wires inserted into the axon are used to measure membrane potential (V) and to pass current (I). The high-gain negative-feedback amplifier compares the command pulse with the membrane potential, and outputs the amount of current necessary to hold the membrane potential constant (or "clamped"). The magnitude of the feedback current can be measured as the IR voltage drop across a resistor and displayed on a cathode-ray oscilloscope (CRO).

Typical records of the membrane current during a voltage clamp experiment. *a* and *c*: In sea water; *b*: in a sodium-free choline chloride solution. (From Hodgkin, 1958, after Hodgkin and Huxley, 1952*a*.)



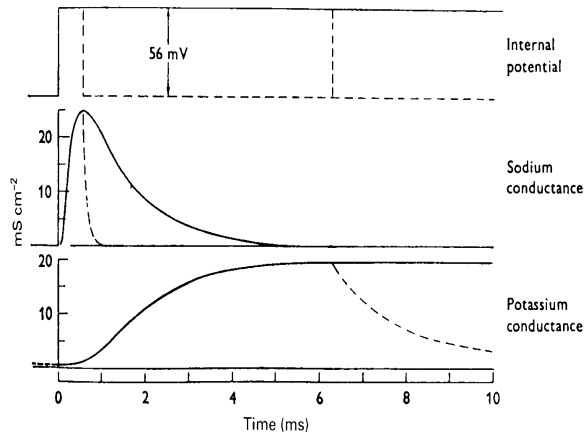


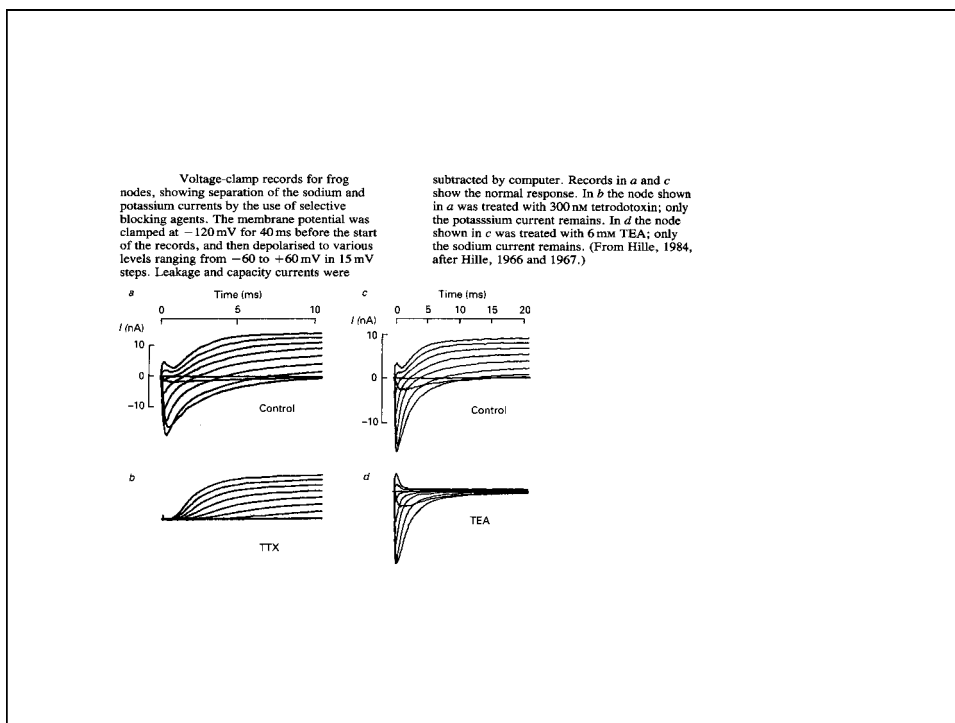
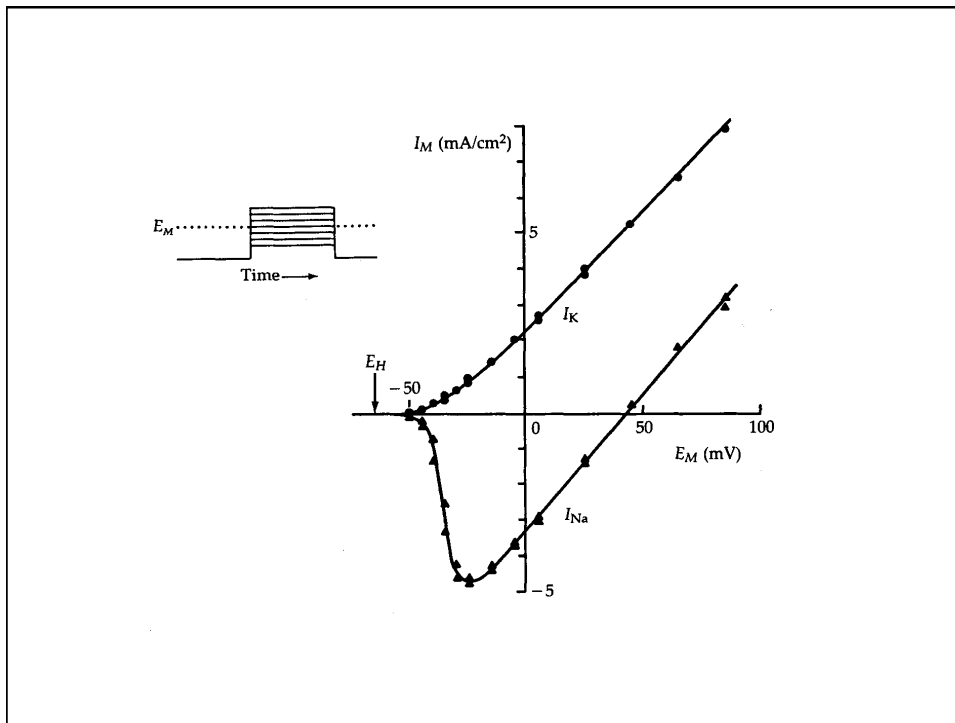


From traces of Na current as a function of time we can obtain g_{Na} by using the equation $I_{Na} = g_{Na}(E - E_{Na})$. E_{Na} is the potential at which the current is nulled.

Ionic conductance changes during a clamped depolarization, derived from the current curves shown in fig. 5.12. The broken

curves show the effects of repolarization. (From Hodgkin, 1958, by permission of the Royal Society.)

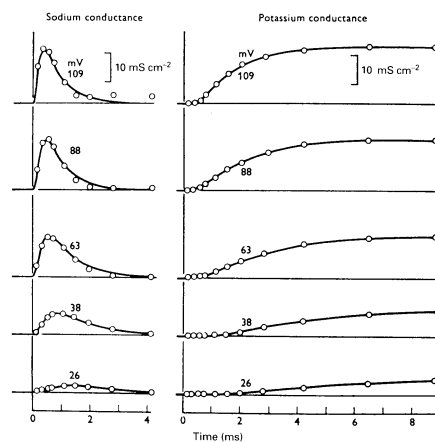




If we knew the time and voltage dependence of g_{Na} and g_K we could obtain the form of the action potential by numerical integration of the following equation.

$$I_m = C_m dV/dt + g_K(E - E_K) + g_{Na}(E - E_{Na}) + g_l(E - E_l)$$

Conductance changes brought about by clamped depolarizations of different extents. The circles represent values derived from the experimental measurements of ionic current, and the curves are drawn according to the equations used to describe the conductance changes. (From Hodgkin, 1958, after Hodgkin and Huxley, 1952d.)



$g_K = \bar{g}_K n^4$ n =probability of 4 charged particles being in the correct configuration for conduction.

$g_{Na} = \bar{g}_{Na} m^3 h$ n =probability of 3 charged particles being in the correct configuration. $1-h$ =probability of inactivation.

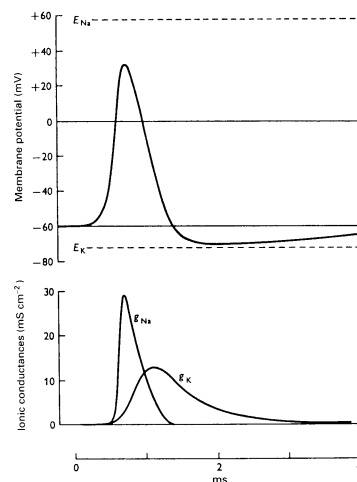
n is the potassium activation parameter, m and h are the Na activation and inactivation parameters.

$$\begin{aligned} I_m &= C_m dE/dt + I_K + I_{Na} + I_i \\ &= C_m dV/dt + g_K(E-E_K) + g_{Na}(E-E_{Na}) + g_i(E-E_i) \\ &= C_m dV/dt + \bar{g}_{Na} n^4 (E-E_K) + \bar{g}_{Na} m^3 h (E-E_{Na}) + g_i(E-E_i) \end{aligned}$$

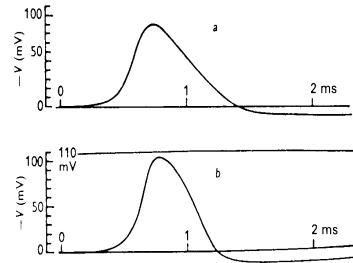
With the voltage and time dependence of m , n and h the Above equation can be solved for V by numerical integration

Calculated changes in membrane potential (upper curve) and sodium and potassium conductances (lower curves) during a propagated action potential in a squid giant axon. The scale of the vertical axis is correct, but its position may be slightly inaccurate; it has been drawn here assuming a resting potential of

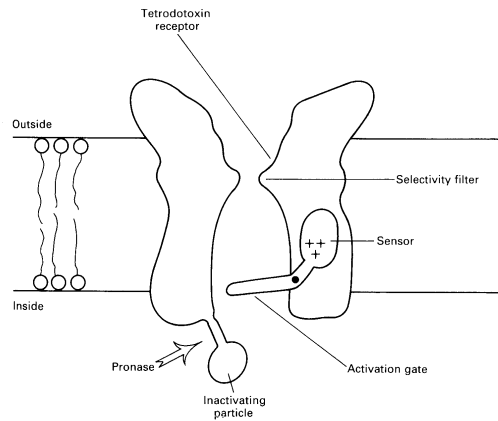
-60 mV. The positions of E_{Na} and E_K are correct with respect to the resting potential. In the original calculations, voltages were measured from the resting potential, as in fig. 5.15. (After Hodgkin and Huxley, 1952; redrawn.)



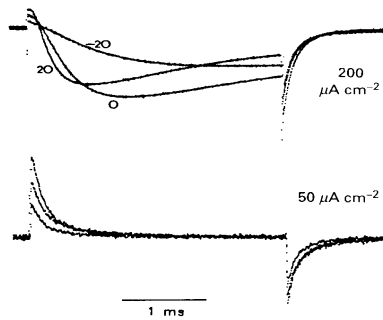
Comparison of computed (a) and observed (b) propagated action potentials in squid axon at 18.5°C. The calculated velocity of conduction was 18.8 m s⁻¹; the observed velocity was 21.2 m s⁻¹. (From Hodgkin and Huxley, 1952d.)



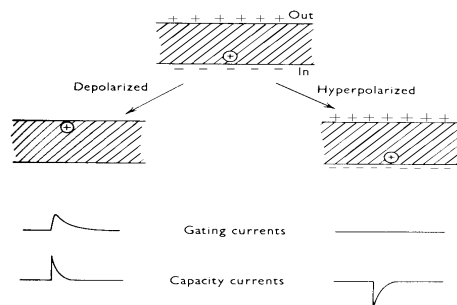
A sketch to show the main features of the sodium channel. (Based partly on diagrams by Armstrong, 1981, and Hille, 1984.)



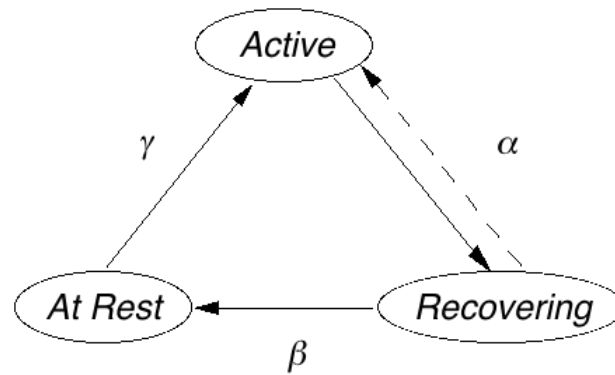
Sodium ionic and gating currents in squid axon, produced during depolarizations under voltage clamp. The upper traces show currents recorded in an artificial sea water with only one fifth of the normal sodium concentration, for depolarizations from -70 mV to -20 , 0 and $+20$ mV. The initial brief outward current is gating current, followed by the much larger inward sodium ionic current. The lower set shows the gating currents alone, after blockage of the sodium ionic currents with tetrodotoxin. Potassium currents were eliminated by using potassium-free solutions for both internal and external media. (From Bezanilla, 1986.)



Schematic diagram showing one way in which gating currents could arise. The capacity currents are much larger than the gating currents.

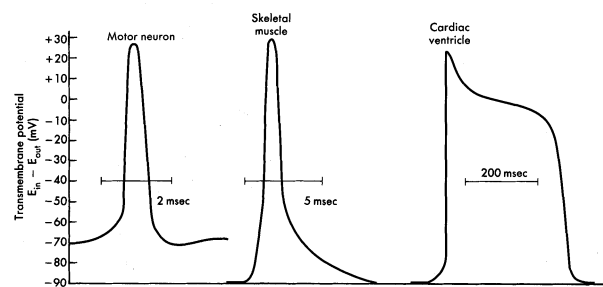


Channel (Gating) Simulations

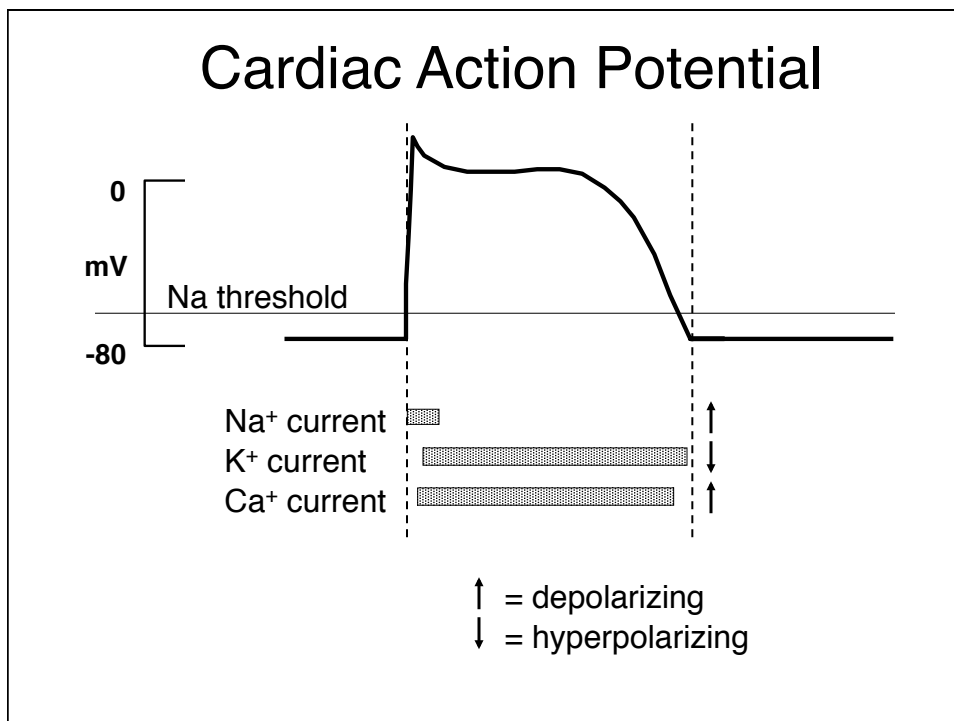
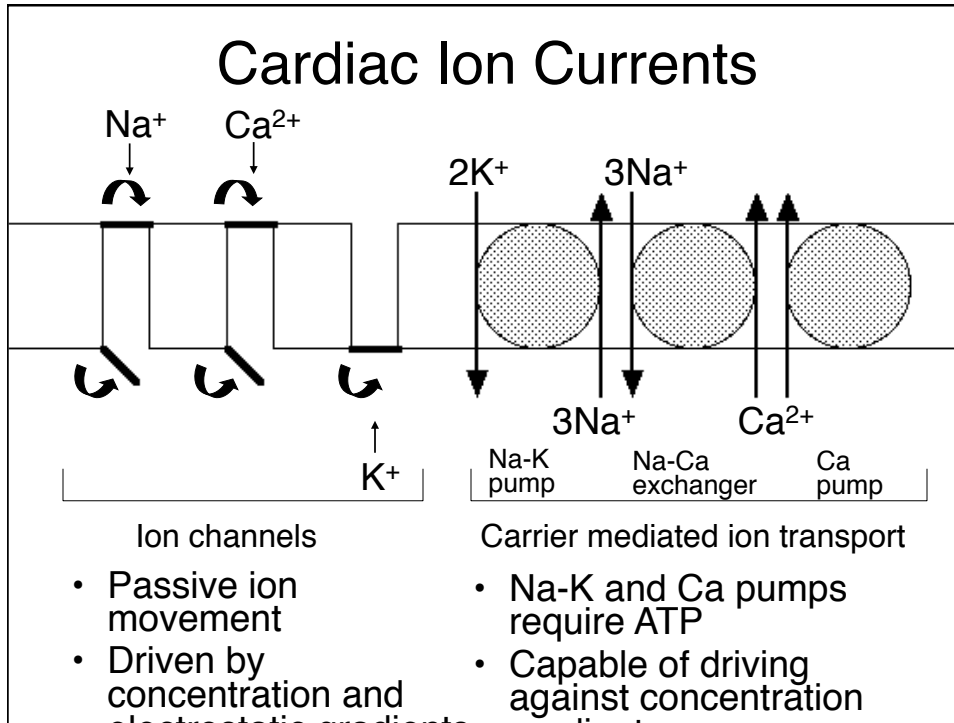


α, β, γ : state transition probabilities,
(functions of v and t)

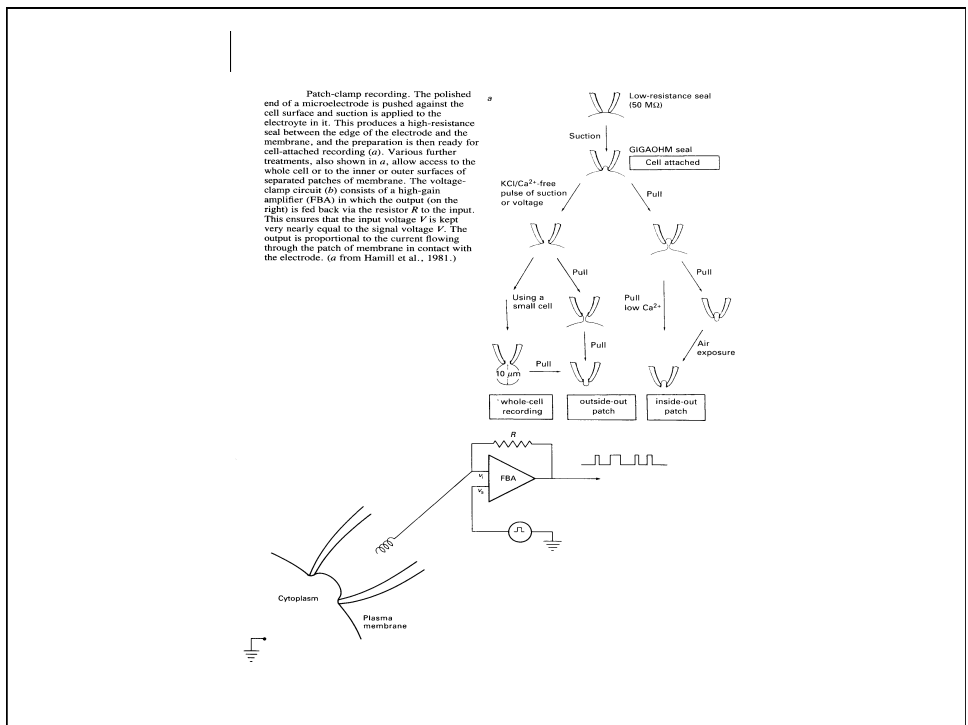
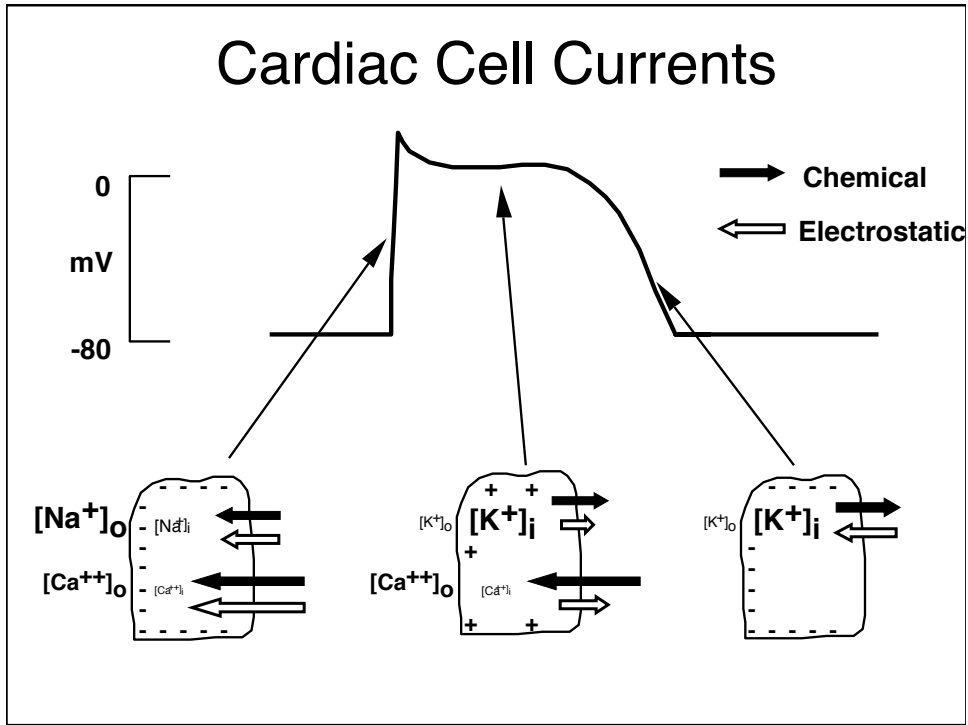
Action Potential from Different Cells



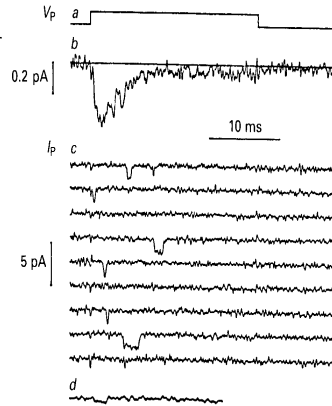
Action potentials from three vertebrate cell types. Note the different time scales.
(Redrawn from Flickinger CJ et al: *Medical cell biology*, Philadelphia, 1979, WB Saunders.)



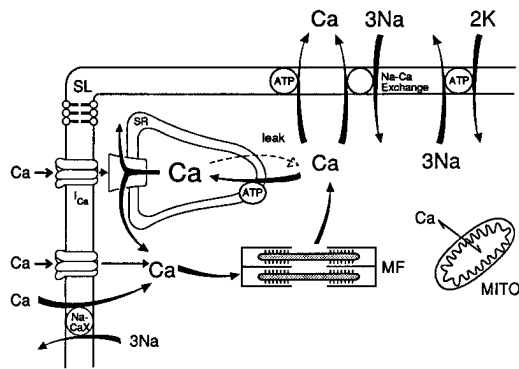
Cardiac Cell Currents



Single sodium channel currents from cultured rat muscle cells, recorded with the cell-attached patch-clamp technique. Trace *a* shows the imposed membrane potential, held at $V = -30$ mV (where $V = 0$ is the resting potential) and depolarized by 40 mV to $V = +10$ mV for about 23 ms at 1 s intervals. Trace *b* shows the average of a set of 300 of current records elicited by these pulses. *c* shows nine successive individual records from this set. Square pulses of inward current (average size 1.6 pA) can be seen in most of the records; these correspond to the opening of individual channels. Trace *d* shows a record taken when two thirds of the sodium ions in the pipette had been replaced with tetramethylammonium ions; the single-channel current is reduced accordingly. (From Sigworth and Neher, 1980.)



Calcium Cycle in Cardiac Muscle



General scheme of Ca cycle in a cardiac myocyte. Ca can enter via Ca channels and Na/Ca exchange. Ca current may also control the SR Ca release by the SR Ca release channel/ ryanodine receptor/ foot protein. Ca is removed from the myofibrils (MF) and cytoplasm by the SR Ca-ATPase pump and the sarcolemmal Ca-ATPase pump and Na/Ca exchange.